UCSF

UC San Francisco Previously Published Works

Authors

Lesman-Segev, Orit H
La Joie, Renaud
Iaccarino, Leonardo
et al.

Diagnostic Accuracy of Amyloid versus ^{18}F-Fluorodeoxyglucose Positron Emission Tomography in Autopsy-Confirmed Dementia

Orit H. Lesman-Segev, MD [1,2] Renaud La Joie, PhD,[1] Leonardo Iaccarino, PhD,[1]

Iryna Lobach, PhD,[3] Howard J. Rosen, MD,[1] Sang Won Seo, MD,[4] Mustafa Janabi, PhD,[5]

Suzanne L. Baker, PhD,[5] Lauren Edwards, BS,[1] Julie Pham, BS,[1] John Olichney, MD,[6]

Adam Boxer, MD,[1] Eric Huang, MD,[1] Marilu Gorno-Tempini, MD,[1] Charles DeCarli, MD,[6]

Mackenzie Hepker, BS,[1] Ji-Hye L. Hwang, PhD,[1] Bruce L. Miller, MD,[1] Salvatore Spina, MD,[1]

Lea T. Grinberg, MD,[1] William W. Seeley, MD,[1] William J. Jagust, MD [5,7]

and Gil D. Rabinovici, MD[1,4,6,8]

Objective: The purpose of this study was to compare the diagnostic accuracy of antemortem ^{11}C-Pittsburgh compound B (PIB) and ^{18}F-fluorodeoxyglucose (FDG) positron emission tomography (PET) versus autopsy diagnosis in a heterogenous sample of patients.

Methods: One hundred one participants underwent PIB and FDG PET during life and neuropathological assessment. PET scans were visually interpreted by 3 raters blinded to clinical information. PIB PET was rated as positive or negative for cortical retention, whereas FDG scans were read as showing an Alzheimer disease (AD) or non-AD pattern. Neuropathological diagnoses were assigned using research criteria. Majority visual reads were compared to intermediate–high AD neuropathological change (ADNC).

Results: One hundred one participants were included (mean age = 67.2 years, 41 females, Mini-Mental State Examination = 21.9, PET-to-autopsy interval = 4.4 years). At autopsy, 32 patients showed primary AD, 56 showed non-AD neuropathology (primarily frontotemporal lobar degeneration [FTLD]), and 13 showed mixed AD/FTLD pathology. PIB showed higher sensitivity than FDG for detecting intermediate–high ADNC (96%, 95% confidence interval [CI] = 89–100% vs 80%, 95% CI = 68–92%, $p = 0.02$), but equivalent specificity (86%, 95% CI = 76–95% vs 84%, 95% CI = 74–93%, $p = 0.80$). In patients with congruent PIB and FDG reads (77/101), combined sensitivity was 97% (95% CI = 92–100%) and specificity was 98% (95% CI = 93–100%). Nine of 24 patients with incongruent reads were found to have co-occurrence of AD and non-AD pathologies.

Interpretation: In our sample enriched for younger onset cognitive impairment, PIB-PET had higher sensitivity than FDG-PET for intermediate–high ADNC, with similar specificity. When both modalities are congruent, sensitivity and specificity approach 100%, whereas mixed pathology should be considered when PIB and FDG are incongruent.

ANN NEUROL 2020;00:1–13

Identifying the etiology of cognitive decline during life is challenging, given imperfect clinical–pathological correspondence.[1,2] Moreover, multiple pathologies are commonly found in older individuals with cognitive impairment, adding diagnostic complexity.[3] Even in expert hands, a clinical diagnosis of Alzheimer disease (AD) based on history and cognitive testing alone (without imaging or biomarker studies) has limited accuracy, with sensitivity ranging between 70.9 and 87.3% and specificity ranging between 44.3 and 70.8% compared with neuropathological diagnosis.[4] The accuracy of a non-AD clinical diagnosis is similarly imperfect. Diagnosing the cause of cognitive impairment is important, as it may help guide management, prognosis, and treatment, and is necessary for clinical trials and future implementation of disease-specific therapies.

Diagnostic accuracy may be improved by introducing imaging biomarkers to the diagnostic workup. Positron emission tomography (PET) with ^{18}F-fluorodeoxyglucose (FDG) and PET with β-amyloid (Aβ) ligands are clinically available modalities in the evaluation of cognitive decline. Amyloid PET has molecular specificity to Aβ plaques (mostly neuritic and to some extent diffuse plaques)[5,6] that are required to define AD neuropathological changes.[7] FDG is a measure of synaptic activity and thus neurodegeneration, and in AD shows a signature pattern of hypometabolism in temporoparietal and posteromedial cortices.[8] Both FDG and amyloid PET demonstrate high accuracy in detecting AD neuropathology. FDG has been previously reported to have >90% sensitivity and 63 to 99% specificity compared with histopathological diagnosis.[9–11] FDG patterns also overlap with regions of tau pathology as measured by PET.[9,10,12] In end-of-life populations, visual interpretation of PET with [^{18}F]-labeled amyloid tracers has shown high sensitivity (88–98%) and specificity (80–95%) in detecting moderate–frequent neuritic amyloid plaques as defined by the Consortium to Establish a Registry for Alzheimer's Disease (CERAD) score.[13–15] Although sensitive and specific in detecting amyloid pathology, amyloid PET may lack specificity for AD, which is defined by the presence of both amyloid plaques and tau neurofibrillary tangles. In a recent multisite study of more clinically relevant populations, ^{11}C-Pittsburgh compound B (PIB) amyloid PET showed 84% sensitivity and 88% specificity in detecting intermediate–high AD neuropathologic change (ADNC), which is considered the threshold for clinically meaningful AD neuropathology.[16] Few studies, however, have directly compared the diagnostic performance of FDG and amyloid PET head to head, and such studies were limited by relatively small samples and the use of clinical (rather than neuropathological) diagnosis as the gold standard.[17–20]

The primary aim of this study was to directly compare the accuracy of PIB amyloid PET and FDG versus neuropathology in well-characterized patients presenting to two academic memory centers. Secondary aims included comparing accuracy in clinical subgroups, comparing inter-rater agreement, assessing the added value of combining both modalities, and evaluating possible explanations for false positive and false negative results for each tracer.

Materials and Methods

Study Design and Participants

We considered 122 consecutive participants enrolled in research studies at one of two tertiary academic memory centers, the University of California, San Francisco (UCSF) Memory and Aging Center (n = 111) or the University of California, Davis (UCD) Alzheimer's Disease Center (n = 11), who had undergone either amyloid or FDG PET during life at Lawrence Berkeley National Laboratory (LBNL) and had a neuropathological assessment between April 2005 and June 2018. UCSF studies recruited cognitively impaired patients referred from the UCSF memory clinic or from other referring clinicians, with an emphasis on early onset dementia (specifically AD and frontotemporal dementia [FTD]).[17] The UCD study recruited both impaired and unimpaired participants from the community, with an emphasis on studying the relationship between vascular risk factors and cognitive outcomes.[21,22] Patients were excluded from the study if they only had imaging with one PET modality (n = 17), if they underwent amyloid PET scan with a tracer other than PIB (n = 3), or if technical issues prevented image processing (n = 1). The final cohort included 101 subjects (93 from UCSF and 8 from UCD). Clinical diagnosis during life was made by dementia specialists based on a multidisciplinary evaluation applying consensus research criteria, blinded to PET results.[23–25] Mild cognitive impairment was attributed to AD (amnestic or nonamnestic AD phenotype) or a non-AD condition (nonamnestic or behavioral presentation consistent with non-AD neuropathology). Figure 1 summarizes the study design. Informed consent was obtained from all subjects or their surrogate decision makers, and the UCSF, UCD, University of California, Berkeley, and/or LBNL Institutional Review Boards for human research approved the study.

Image Acquisition

PET scans were conducted between May 2005 and March 2016 at LBNL on a Siemens (Erlangen, Germany) ECAT EXACT HR PET scanner (n = 91) or Siemens Biograph 6 Truepoint PET/CT scanner (n = 10) in 3-dimensional acquisition mode.[26] FDG and PIB were obtained on the same day for 95 participants with a median of 186 days between the two scans (range = 97–441 days) for the other 6 patients. A low-dose computed tomography (CT) scan was performed for attenuation correction prior to the Siemens Biograph 6 Truepoint PET/CT scans, and a 10-minute transmission scan for attenuation correction was obtained for Siemens ECAT EXACT HR PET scans.
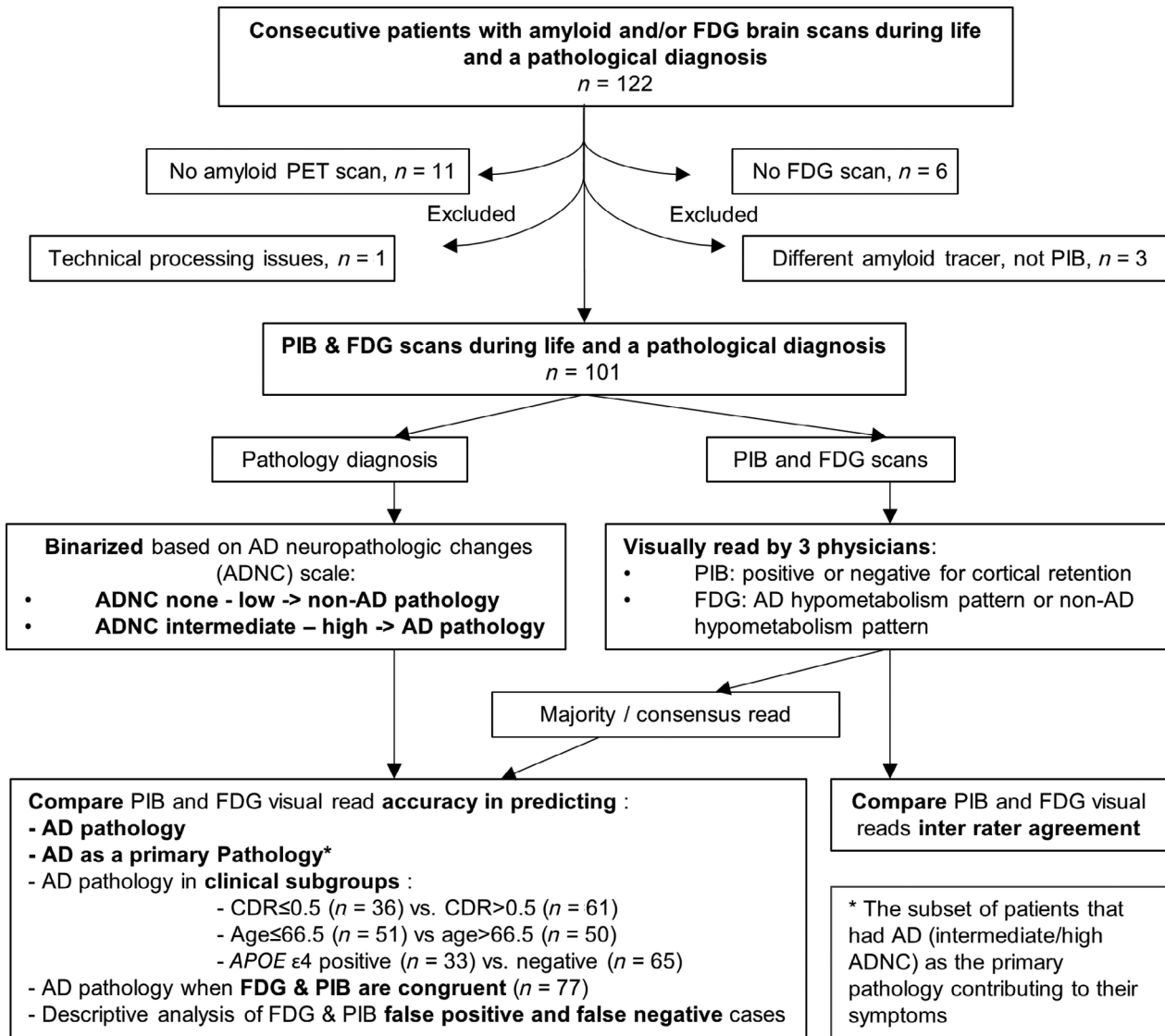
FIGURE 1: Study design. AD = Alzheimer disease; ADNC = AD neuropathological change; *APOE* ε4 = apolipoprotein E ε4; CDR = Clinical Dementia Rating; FDG = ^{18}F-fluorodeoxyglucose; PET = positron emission tomography; PIB = ^{11}C-Pittsburgh compound B.

PIB was synthesized at the LBNL Biomedical Isotope Facility. FDG was purchased from a commercial vendor (IBA Molecular, Sanford, FL). Injected doses were approximately 15mCi for PIB and 5 to 10mCi for FDG. We analyzed data acquired from 90-minute or 20-minute PIB scans (0–90 or 50–70 minutes postinjection) and 30-minute FDG scans (30–60 minutes postinjection).

Image Processing

Ninety-seven of 101 subjects underwent structural T1-weighted magnetic resonance imaging (MRI). Scans were obtained on different MRI units, including three 1.5T units (Magnetom Avanto System, Siemens Medical Systems, Erlangen, Germany; Magneton VISION system, Siemens, Iselin, NJ; or SYGNA, GE Healthcare, Chicago, IL), two 3T units (Siemens Tim Trio/Prisma scanners), and one 4T unit (MEDSPEC, Bruker, Billerica, MA) at the UCSF neuroimaging center or the UCD Imaging Research Center. Acquisition parameters for all scanners have been previously described.[23,27] MRI was used for PET image preprocessing only. PET frames were realigned, averaged, and coregistered onto their corresponding T1 MRI. T1 MRI images were parcellated using FreeSurfer 5.3 (surfer.nmr.mgh.harvard.edu). We calculated PIB standard uptake value ratio (SUVR) using the cerebellar gray matter (defined on the MRI) as the reference region. When 90-minute acquisition was available, we also generated PIB distribution volume ratio (DVR) images using Logan graphical analysis with cerebellar gray matter as the reference region. FDG SUVR images were created using the pons (defined on the MRI) as a reference region.[28–30]

Visual Reads

SUVR FDG images and DVR PIB (n = 81) or SUVR PIB (when DVR was not available, n = 16) images were read separately by 3 experienced physicians (2 neurologists and

1 radiologist) blinded to all clinical information. For the 4 patients who did not have available MRI, PET images reflecting summed activity (PIB: 50–70 minutes, FDG: 30–60 minutes postinjection) were read. PIB and FDG images were read in MRICron software using the National Institutes of Health color scale (similar to "rainbow") in the axial plane, with optional coronal and sagittal plans used mainly for medial parietal cortices and temporal cortex. Clinicians were free to window the color scale to optimize gray/white matter contrast in the cerebellum (for PIB), and to optimize the visualization of metabolic patterns for FDG. PIB was read as positive if cortical binding equaled or exceeded white matter binding in one or more regions.[17] FDG scans were read as showing an AD-like hypometabolism pattern, defined as posterior cingulate/precuneus and/or lateral temporoparietal predominant hypometabolism, or a non-AD pattern, defined as anything other than the AD pattern, including normal metabolism or abnormal metabolism that is not consistent with AD.[31] Individual rater reads were aggregated into consensus (3/3 raters agree) or majority (2/3 raters agree) reads for each modality in each patient (Fig 2).

Neuropathological Evaluation

Neuropathological diagnoses were based on brain autopsy (n = 100) or brain biopsy (n = 1,[32] patient with atypical corticobasal syndrome with concern for inflammatory etiology, biopsy revealed corticobasal degeneration). Deaths occurred between February 2006 and December 2017. Brain autopsies were performed at UCSF (n = 88), UCD (n = 8), University of Pennsylvania (n = 2), University of California, Los Angeles (n = 1), and Mayo Clinic Jacksonville (n = 1). Pathologic assessments were performed using institution-specific protocols as previously described.[16,17,33,34] All autopsies included tissue sampling in regions relevant to the differential diagnosis of dementia based on published consensus criteria.[35,36] Tissue staining included some combination of hematoxylin and eosin, silver staining with modified Bielschowsky or Gallyas methods, and immunohistochemistry for amyloid-beta, hyperphosphorylated tau, α-synuclein, and TDP-43.

Neuropathologists were blinded to PET findings but not to the patient's clinical history. AD-related changes were scored according to the Thal amyloid phase,[37] Braak neurofibrillary tangle stage,[38] and CERAD neuritic plaque score.[39] Overall severity of ADNC was assigned using the National Institute on Aging (NIA)–Reagan criteria and NIA–Alzheimer Association criteria for AD.[36] ADNC levels were further dichotomized into none-to-low versus intermediate-to-high ADNC. Intermediate-to-high ADNC was defined as consistent with clinically significant AD pathology. We further noted whether AD pathology was considered by the evaluating neuropathologist as the primary cause of cognitive impairment ("primary pathology") or as a "contributing pathology." "Primary pathology" was defined as the main pathology believed to explain the patient's clinical picture based on its location and burden in relation to the symptoms. A "contributing pathology" was defined as a pathology believed to explain some of the patient's symptoms, with an alternative

pathology (eg, frontotemporal lobar degeneration) identified as primary. In this cohort, intermediate-to-high ADNC was always deemed to represent at least a contributing pathology.

Comparison of Visual Reads to Pathological Diagnosis

Both consensus/majority and individual rater PET scan reads were compared to AD neuropathology, that is, intermediate-to-high ADNC (see Fig 2). The primary analysis compared the diagnostic performance (sensitivity, specificity, positive/negative predictive values, positive/negative likelihood ratios, and overall accuracy) of FDG and PIB in detecting AD neuropathology. Secondary analysis included comparison of FDG and PIB in identifying AD as the "primary pathology" underlying cognitive decline, and comparison of the diagnostic accuracy of PIB and FDG in clinically relevant subgroups: (1) early versus late disease stage based on a Clinical Dementia Rating (CDR) threshold of 0.5, (2) younger versus older patients (split by cohort median age of 66.5 years), and (3) apolipoprotein E (*APOE*) ε4 carriers versus noncarriers. We additionally assessed the added value of combining both modalities together rather than assessing each modality separately, that is, the diagnostic utility when PIB and FDG were congruent. Finally, we compared PIB and FDG inter-rater agreement, and investigated possible causes for false positive/negative reads.

Statistical Analysis

Diagnostic performance of FDG and PIB was characterized by evaluating overall accuracy, sensitivity, specificity, positive and negative predictive values, and positive and negative likelihood ratios. PIB accuracy was defined as (n patients with ADNC intermediate–high at autopsy read as PIB positive + n patients with ADNC no–low at autopsy read as PIB negative)/n total. FDG accuracy was defined in analogous fashion. Statistical analyses were performed with R (v4.0.0, www.R-project.org). Sensitivity/specificity, positive/negative likelihood ratios, positive/negative predictive values, overall accuracy, and respective 95% confidence intervals (CIs) were estimated for individual biomarkers with the *DTComPair*[40] and *caret*[41] packages. Paired analyses were adopted to compare diagnostic performances for PIB and FDG given their dependency. Sensitivities and specificities were compared by means of a McNemar test, whereas positive/negative likelihood ratios were compared with a regression model approach[42] and positive/negative predictive values were compared with a generalized score statistic,[43] all implemented in the *DTComPair* package. Differences in accuracy, in terms of relative proportion of errors, were tested with a McNemar test.

To account for possible effects of the PET-to-autopsy interval, logistic regression analyses were separately run for both PIB and FDG, adding the time interval to the models. The respective fitted values were then used as predictors after being binarized. The threshold adopted to binarize the fitted values was selected using a bootstrapping approach (n = 1,000 replicates) to select the cut point maximizing the Youden index with the cutpointr R package.[44] Diagnostic accuracy measures for the binarized fitted value vectors were assessed as described above.
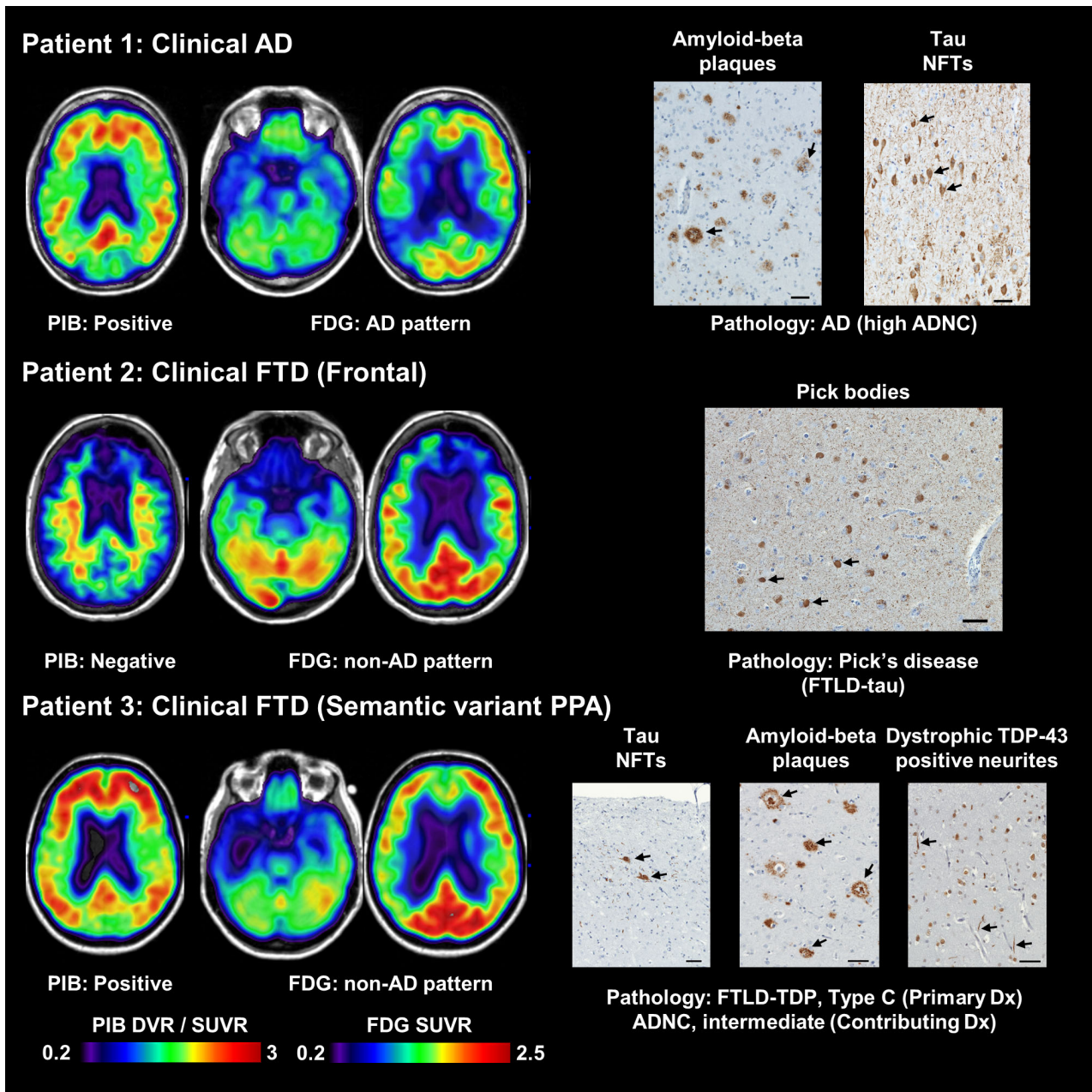
FIGURE 2: ^{11}C-Pittsburgh compound B (PIB), ^{18}F-fluorodeoxyglucose (FDG), and pathology in representative patients: Patient 1 had a clinical diagnosis of Alzheimer disease (AD), a positive PIB scan, and an AD pattern of hypometabolism on FDG. Selected pathological slices from the hippocampus show neurofibrillary tangles (NFTs), tau-positive neurites and threads, and amyloid-beta plaques. Pathological diagnosis was AD with high AD neuropathologic change (ADNC). Patient 2 had a clinical diagnosis of behavioral variant frontotemporal dementia (FTD), a negative PIB scan, and a non-AD pattern of hypometabolism on FDG. A selected pathological slice from the amygdala stained for tau shows Pick bodies. Pathological diagnosis was Pick disease. Patient 3 had a clinical diagnosis of semantic-variant primary progressive aphasia (PPA). PIB was positive, and a non-AD pattern of hypometabolism was seen on FDG. Selected pathological slices show NFTs and threads in hippocampus, amyloid plaques in superior/middle temporal gyrus, and TAR DNA-binding protein (TDP)-43–positive dystrophic neurites in anterior cingulate cortex. Primary pathological diagnosis was frontotemporal lobar degeneration (FTLD)-TDP-43, type C, and the contributing pathology was AD with intermediate ADNC. Immunohistochemical preparations are shown with original magnification, ×20. Scale bars indicate 100μm. DVR = distribution volume ratio; Dx = diagnosis; SUVR = standardized uptake value. Images are presented in neurological convention (left of the image is the left side of the patient).

Agreement in classifying scans across 3 raters was estimated by percent agreement and Fleiss kappa statistic. To test for incremental diagnostic performance in adding FDG to PIB or vice versa, separate logistic regression models were fit as basic (FDG or PIB as standalone imaging), and as incremental (FDG and PIB or PIB and FDG), for detecting AD as primary/contributing pathology. Incremental value was tested by means of a log likelihood ratio test for nested logistic regression models with the rms R package.[45]

Role of the Funding Source

The funders of the study had no role in study design, data collection, data analysis, data interpretation, or writing of the paper. The corresponding author had full access to all the data in the study and had final responsibility for the decision to submit for publication.

Results

Participants

Cohort characteristics are summarized in Table 1. The average age at PET was 67 years (range = 42–90), and there was a preponderance of males (60/101). At the time of PET, most patients met clinical criteria for either AD or a non-AD dementia (most commonly the FTD spectrum; Table 2). PET to autopsy interval was 4.4 years on average (range = 0.2–11.6 years). Most patients had either high (n = 36) or none-to-low ADNC (n = 50). Correlations between clinical and pathological diagnoses are shown in Table 2.

PIB versus FDG: Accuracy in Detecting AD

Based on majority reads, PIB demonstrated significantly better sensitivity (96%, 95% CI = 89–100% vs 80%, 95% CI = 68–92% for FDG, *p* = 0.02), negative likelihood ratio (0.05, 95% CI = 0.01–0.2 vs 0.24, 95% CI = 0.13–0.43 for FDG, *p* = 0.03), and negative predictive value (96%, 95% CI = 91–100% vs 84%, 95% CI = 74–93% for FDG, *p* = 0.01) in detecting intermediate-high ADNC (Table 3, A). There were no differences between modalities in specificity, positive likelihood ratio, and positive predictive value. PIB and FDG majority reads showed equivalent performance in detecting intermediate–high ADNC as the primary pathology underlying clinical impairment (see Table 3, B).

After adjusting the models for the PET-to-autopsy interval, the sensitivity and specificity of PIB in detecting intermediate–high ADNC were not changed (96%, 95% CI = 89–100% and 86%, 95% CI = 76–95%, respectively), whereas for FDG sensitivity decreased to 78% (95% CI = 66–90%) and specificity increased to 89% (95% CI = 81–97%). The performance of the 3 raters was similar, with accuracy of 89% (95% CI = 80–98%), 96% (95% CI = 89–100%), and 100% (95% CI = 100–100%) for each of the 3 raters for PIB reads, and 79% (95% CI = 70–89%; identical for all 3 raters) for FDG visual reads.

PIB versus FDG: Inter-Rater Agreement

Consensus visual reads (full agreement between raters) occurred for 84 of 101 PIB scans and 72 of 101 FDG scans. Inter-rater agreement was higher for PIB (Fleiss kappa = 0.77, 95% CI = 0.68–0.87) than FDG (kappa = 0.61, 95% CI = 0.49–0.73, *p* = 0.03).

PIB versus FDG: Accuracy in Detecting AD, Subgroup Analysis

Supplementary Table S1 shows the accuracy of PIB and FDG in detecting AD pathology (ie, intermediate-to-high ADNC as primary or contributing causative pathology) in clinically relevant patient subgroups. PIB demonstrated significantly higher sensitivity (100%, 95% CI = 79–100% vs 69%, 95% CI = 46–91% for FDG, *p* = 0.03), negative likelihood ratio (0 vs 0.39, 95% CI = 0.18–0.84 for FDG, *p* = 0.03), and negative predictive value (100%, 95% CI = 83–100% vs 79%, 95% CI = 63–95% for FDG, *p* = 0.01) when assessing patients in early symptomatic stages (CDR ≤ 0.5). No significant difference was found in patients with more advanced disease stage (CDR > 0.5). There were only trend differences between PIB and FDG when patients were dichotomized by age at scan. In younger patients (≤66.5 years) PIB was both highly sensitive (100%, 95% CI = 85–100% vs 91%, 95% CI = 71–99% for FDG, *p* = 0.16) and specific (93%, 95% CI = 77–99% vs 79%, 95% CI = 60–92%, *p* = 0.16). In *APOE* ε4 carriers, the specificity of PIB was 70% (95% CI = 35–93%), nominally but not statistically lower than FDG (90%, 95% CI = 55–100%, *p* = 0.32). In patients with longer PET-to-autopsy intervals (greater than the median 3.9 years), PIB demonstrated higher sensitivity (96%, 95% CI = 82–100% vs 75%, 95% CI = 55–89%, *p* = 0.01), lower negative likelihood ratio (0.04, 95% CI = 0.01–0.3 vs 0.27, 95% CI = 0.14–0.52, *p* = 0.042), higher negative predictive value (95%, 95% CI = 76–100% vs 76%, 95% CI = 56–90%, *p* = 0.008), and higher total accuracy (92%, 95% CI = 80–98% vs 83, 95% CI = 68–91%, *p* = 0.04). No difference between the modalities was found in patients with shorter PET-to-autopsy intervals (≤3.9 years; Table 4).

Combining PIB and FDG

PIB and FDG were congruent in suggesting AD or non-AD diagnoses in 77 of 101 patients (eg, Patients 1 and 2; see Figs 2 and 3). The overall accuracy in detecting AD pathology was 97% (95% CI = 91–100%) when scans were congruent (sensitivity = 97%, 95% CI = 92–100%; specificity = 98%, 95% CI = 93–100%). In 15 patients, PIB was positive but FDG suggested a non-AD pathology (eg, Patient 3; see Fig 2) and in 9 patients, PIB was negative and FDG suggested AD. Nine of the 24 discordant patients were found to have mixed AD and non-AD pathologies. In the remaining 15 discordant patients, the underlying pathology was accurately predicted by PIB in 8 patients and by FDG in 7. Comparing the area under the curve (AUC) for each of the traces individually to the combination of the two

Demographics	Total, n = 101	AD Autopsy Diagnosis, n = 32[a]	Non-AD Autopsy Diagnosis, n = 56[a]	Mixed AD & Non-AD Autopsy Diagnosis, n = 13[b]	p[c]
TABLE 1. Study Population					
Age at PET, yr	67.2 ± 9.3 [42.1–89.9]	65.3 ± 10.1 [51.4–89.9]	67.6 ± 9.5 [42.1–87.9]	70.2 ± 5.4 [63.5–82.8]	0.08
Sex, M/F, n	60/41	21/11	34/22	5/8	0.23
Education, yr	15.8 ± 2.7 [12–22]	16.5 ± 2.6 [12–22]	15.7 ± 2.6 [12–21]	15.3 ± 2.8 [12–20]	0.23
Race, Asian/Black/ mixed/White/missing, n	4/1/2/85/9	0/0/0/30/2	4/1/1/43/7	0/0/1/12/0	0.43
Clinical characteristics					
Clinical diagnosis: normal/AD/non-AD[d]	3/34/64	0/29/3	3/3/50	0/2/11	<0.001
MMSE at PET	21.9 ± 6.6 [1–30]	18.0 ± 6.8 [1–28]	23.8 ± 5.7 [3–30]	23.3 ± .8 [12–30]	<0.001
CDR at PET, 0/0.5/1/2/3, n[e]	9/27/43/13/5	0/7/18/4/1	7/15/20/9/3	2/5/5/0/1	0.28
APOE ε4 alleles, 0/1/2, n[e]	65/25/8	14/11/4	46/8/2	5/6/2	<0.001
Neuropathological characteristics					
PET-to-autopsy interval, yr	4.4 ± 2.6 [0.2–11.6]	5.6 ± 2.6 [0.7–11.6]	3.7 ± 2.5 [0.2–10]	4.4 ± 2.7 [1–8.3]	<0.001
ADNC, none/low/ intermediate/high, n[e]	18/32/8/36	0/0/1/30	18/32/0/0	0/0/7/6	

Continuous variables are presented as average ± standard deviation [minimum–maximum].

[a]Pathological diagnosis of AD includes AD only, and AD with vascular disease, Lewy body disease, or cerebral amyloid angiopathy (pathologies that commonly co-occur with AD). Pathological diagnosis of non-AD includes FTLD-tau, FTLD–TDP-43, FTLD–TDP-43–motor neuron disease, vascular disease, chronic traumatic encephalopathy, familial Creutzfeldt–Jakob disease, argyrophilic grain disease, and tangle only AD.

[b]In mixed pathology, AD (intermediate–high ADNC) can be a primary or contributing pathology.

[c]Kruskal–Wallis analysis of variance for all continuous variables, chi-squared for nominal and ordinal variables.

[d]Clinical diagnosis of AD includes AD and AD–Lewy body dementia (including MCI or dementia most likely due to early AD pathology). Clinical diagnoses of non-AD (includes MCI or dementia most likely due to early non-AD pathology) include corticobasal syndrome, nonfluent/agrammatic primary progressive aphasia, semantic-variant primary progressive aphasia, behavioral variant FTD, FTD–amyotrophic lateral sclerosis, progressive supranuclear palsy, Lewy body dementia, vascular dementia, prion disease, and traumatic encephalopathy syndrome.

[e]CDR score is not available for 4 patients, *APOE* genotype is not available for 3 patients, and ADNC score is not available for 7 patients.

AD = Alzheimer disease; ADNC = AD neuropathological change; *APOE* ε4 = apolipoprotein E ε4; CDR = clinical dementia rating; F = female; FTD = frontotemporal dementia; FTLD = frontotemporal lobar degeneration; M = male; MCI = mild cognitive impairment; MMSE = Mini-Mental State Examination; PET = positron emission tomography; TDP = tar DNA binding protein.

tracers, we found a significant difference, with AUC increasing from 0.820 (95% CI = 0.743–0.896) to 0.960 (95% CI = 0.923–0.997) when adding PIB to FDG (χ^2 = 47.90, $p < 0.001$), and from 0.906 (95% CI = 0.851–0.962) to 0.960 (95% CI = 0.923–0.997) when adding FDG to PIB (χ^2 = 14.59, $p < 0.001$).

Possible Explanations for False Positive and False Negative Reads

False negative PIB and FDG scans tended to have longer PET-to-autopsy intervals (Supplementary Tables S2 and S3). Comorbid frontotemporal lobar degeneration (primary) and AD (contributing) was found in 7 of 9 false

TABLE 2. Clinical to Pathological Diagnosis Correlation

Clinical/Path	AD Only Path	Mixed Path (AD & non-AD)	Pick Disease (FTLD-tau)	CBD (FTLD-tau)	PSP (FTLD-tau)	FTLD–TDP-43	Vascular	Other	Total
AD clinical	28	2		1		1		2	34
PSP		1		1					2
CBS	3	5	1	5	1	1		1	17
bvFTD			4	3		2		1	10
FTD-ALS						5			5
nfvPPA		2	3	5	2	1			13
svPPA		3	1			6			10
LBD								1	1
Vascular dementia	1						3		4
famCJD								1	1
TES								1	1
Normal						1	1	1	3
Total	32	13	9	15	3	17	4	8	101

Other pathological diagnoses include argyrophilic grain disease, nonspecific 4R tauopathy, Creutzfeldt–Jakob disease, chronic traumatic encephalopathy, and normal aging.

AD = Alzheimer disease; bvFTD = behavioral variant frontotemporal dementia; CBD = corticobasal degeneration; CBS = corticobasal syndrome; famCJD = familial Creutzfeldt–Jakob disease; FTD-ALS = frontotemporal dementia–amyotrophic lateral sclerosis; FTLD = frontotemporal lobar degeneration; LBD = Lewy body dementia; nfvPPA = nonfluent/agrammatic primary progressive aphasia; Path = pathology; PSP = progressive supranuclear palsy; svPPA = semantic-variant primary progressive aphasia; TDP = tar DNA binding protein; TES = traumatic encephalopathy syndrome.

negative FDG cases. High amyloid burden with low Braak stage (classified as "low ADNC") characterized the majority of false positive PIB cases, whereas corticobasal degeneration was the causative pathology in 5 of 9 cases with false positive FDG (see Supplementary Tables S2 and S3).

Discussion

In this study, we directly compared the diagnostic accuracy of visual interpretation of amyloid (PIB) and FDG PET in a heterogeneous memory clinic population with autopsy-confirmed diagnoses. We found that both PET modalities showed overall high accuracy, although PIB had higher sensitivity, negative likelihood ratio, and negative predictive value compared to FDG in detecting AD pathology. PIB and FDG performed comparably in detecting AD as the primary pathology underlying cognitive decline. The high sensitivity and negative predictive value of PIB in our work suggest that amyloid PET may be a suitable imaging modality for the detection of AD (rather than solely amyloidosis) and validate the approach many clinicians take when changing patient management based on amyloid PET results.[46]

PIB had higher sensitivity and negative predictive value than FDG for the presence of intermediate–high ADNC, but had similar specificity and positive predictive value, and was equally sensitive to FDG in detecting AD as the primary causative pathology. It is broadly recognized that AD has a long preclinical phase, and ADNC is found in a significant proportion of cognitively normal individuals.[47] Therefore, although amyloid PET reliably detects amyloid pathology (and in our study intermediate-to-high ADNC in general), a positive amyloid PET is less clearly linked to the clinical presentation and may represent merely a contributing factor in individuals suffering from a different primary cause of neurodegeneration. In contrast, hypometabolism on FDG reflects reduction in synaptic activity and neurodegeneration. Although hypometabolism is not process specific, the pattern of hypometabolism represents the differential involvement of specific functional networks and thus is highly related to clinical phenotype, which in turn is probabilistically related to underlying neuropathology.[26,48] This may explain why FDG performs particularly well in identifying AD as the primary cause of cognitive impairment (reflecting clinical involvement of

TABLE 3. Diagnostic Utility in Detecting Intermediate–High ADNC or Intermediate-High ADNC as Primary Pathology

	A. Intermediate–High ADNC n=101, 45 I/H ADNC			B. AD as Primary Pathology n=101, 34 I/H ADNC Primary Pathology		
	PIB	FDG	p	PIB	FDG	p
Sensitivity, %	96 [89–100]	80 [68–92]	0.02[a]	97 [91–100]	94 [86–100]	0.31
Specificity, %	86 [76–95]	84 [74–93]	0.80	73 [62–84]	81 [71–90]	0.30
Positive likelihood ratio	6.7 [3.5–12.7]	5 [2.7–9.2]	0.52	3.6 [2.4–5.4]	4.8 [3–8]	0.35
Negative likelihood ratio	0.05 [0.01–0.2]	0.24 [0.13–0.43]	0.03[a]	0.04 [.01–0.28]	0.07 [0.02–0.28]	0.40
Positive predictive value, %	84 [74–94]	80 [68–92]	0.53	65 [52–78]	71 [58–84]	0.34
Negative predictive value, %	96 [91–100]	84 [74–93]	0.01[a]	98 [94–100]	96 [92–100]	0.38
Accuracy, %	90 [83–95]	82 [73–89]	0.15	81 [72–88]	85 [77–91]	0.54

Diagnostic utility of PIB and FDG in (A) detecting the presence of AD pathology (I/H ADNC as the primary or secondary pathological diagnosis); and (B) detecting AD (I/H ADNC) as the primary pathological diagnosis.
Diagnostic utility is presented as percentage [95% confidence interval].
[a]Statistically significant.
AD = Alzheimer disease; ADNC = AD neuropathological change; FDG = ^{18}F-fluorodeoxyglucose; I/H = intermediate/high; PIB = ^{11}C-Pittsburgh compound B.

susceptible posterior cortical networks), but shows lower overall accuracy in detecting the presence or absence of ADNC (which may not yet manifest a functional impact on synaptic activity or brain metabolism or may be obscured by the co-occurrence of other substantial neuropathologies involving more anterior networks). These observations are further supported by a subgroup analysis, which revealed that PIB was more sensitive than FDG in early disease stages (CDR ≤ 0.5), when amyloid deposition is typically diffuse, but functional changes may be subtle. Therefore, when assessing a patient with mild clinical symptoms, amyloid PET is a more sensitive imaging choice for detecting AD, but when assessing patients later in the course of disease with overt clinical symptoms, amyloid PET and FDG have similar diagnostic properties.

TABLE 4. Accuracy with Shorter (≤3.9 Years) and Longer (>3.9 Years) PET-to-Autopsy Time Interval

PET to Autopsy Interval	Shorter (≤3.9 yr) n = 50, 17 I/H ADNC			Longer (>3.9 yr) n = 51, 28 I/H ADNC		
	PIB	FDG	p	PIB	FDG	p
Sensitivity	94 [71–100]	88 [64–99]	0.56	96 [82–100]	75 [55–89]	0.01[a]
Specificity	85 [68–96]	78 [60–91]	0.32	87 [66–97]	92 [73–99]	0.65
Positive likelihood ratio	6.2 [2.8–14.1]	4.0 [2.1–7.9]	0.28	7.4 [2.6–21.3]	9 [2.4–34.5]	0.61
Negative likelihood ratio	0.07 [0.01–0.45]	0.15 [0.04–0.56]	0.51	0.04 [0.01–0.3]	0.27 [0.14–0.52]	0.04[a]
Positive predictive value	76 [53–92]	68 [45–86]	0.27	90 [73–98]	91 [72–99]	0.87
Negative predictive value	97 [82–100]	93 [76–99]	0.51	95 [76–100]	76 [56–90]	0.01[a]
Accuracy	88 [76–95]	82 [68–91]	0.77	92 [80–98]	83 [68–91]	0.04[a]

[a]Statistically significant.
ADNC = Alzheimer disease neuropathological change; FDG = ^{18}F-fluorodeoxyglucose; I/H = intermediate/high; PET = positron emission tomography; PIB = ^{11}C-Pittsburgh compound B.
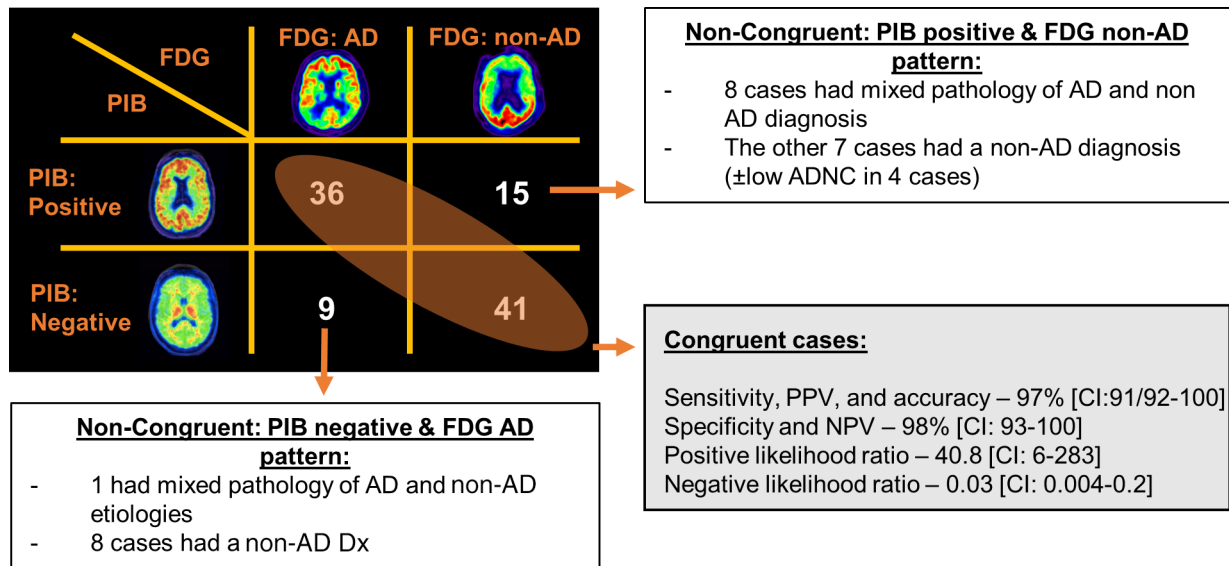
Non-Congruent: PIB positive & FDG non-AD pattern:
- 8 cases had mixed pathology of AD and non AD diagnosis
- The other 7 cases had a non-AD diagnosis (±low ADNC in 4 cases)

Non-Congruent: PIB negative & FDG AD pattern:
- 1 had mixed pathology of AD and non-AD etiologies
- 8 cases had a non-AD Dx

Congruent cases:

Sensitivity, PPV, and accuracy – 97% [CI:91/92-100]
Specificity and NPV – 98% [CI: 93-100]
Positive likelihood ratio – 40.8 [CI: 6-283]
Negative likelihood ratio – 0.03 [CI: 0.004-0.2]

FIGURE 3: Agreement between ^{11}C-Pittsburgh compound B (PIB) and ^{18}F-fluorodeoxyglucose (FDG) reads. AD = Alzheimer disease; ADNC = AD neuropathologic change; CI = 95% confidence interval; Dx = diagnosis; NPV = negative predictive value; PPV = positive predictive value.

Amyloid PET evaluates the deposition of amyloid plaques. Nevertheless, we found that PIB had high sensitivity and specificity for intermediate–high ADNC, indicating the presence of both plaques and tau tangles. Two factors probably contribute to this finding: (1) in this cohort of (on average) young and cognitively impaired individuals, isolated/incidental amyloidosis is rare; and (2) amyloid PET positivity corresponds with an intermediate or high overall burden of amyloid pathology (Thal phase ≥ 2–3, CERAD moderate–frequent neuritic plaques),[16] at which point significant tau pathology and overall intermediate–high ADNC are likely.[49]

A trend toward improved performance of PIB compared with FDG was seen in patients younger than 66.5 years. In this age group, PIB was both highly sensitive (100%, 95% CI = 85–100%) and highly specific (93%, 95% CI = 77–99%). Patients with early onset AD typically have more severe AD neuropathology and less mixed pathology[50]; thus, false negative rates are likely to be low. The high specificity likely reflects a lower prevalence of incidental amyloidosis in younger patients.[51]

In *APOE* ε4 carriers, PIB was sensitive for AD pathology (96%, 95% CI = 78–100%) but showed low specificity (70%, 95% CI = 35–93%) compared to performance in non–ε4-carriers (89%, 95% CI = 76–96%). *APOE* ε4 is known to be associated with higher rates of amyloid deposition at all ages regardless of clinical state or syndrome.[51] Thus, the clinical significance of a positive amyloid scan should be interpreted with caution in *APOE* ε4 carriers, especially if the clinical presentation suggests a non-AD dementia.

Appropriate use criteria for amyloid PET have been published[52] representing expert opinion on the clinical scenarios in which amyloid PET is suitable as part of the diagnostic workup. These criteria include (1) persistent or progressive unexplained mild cognitive impairment and (2) progressive dementia with atypically early age at onset (<65 years old). The high diagnostic performance of PIB in patients with CDR ≤ 0.5 and in patients younger than 66.5 years in this study reinforces the utility of amyloid PET in these populations.

Sensitivity and specificity approached 100% when PIB and FDG were congruent, whereas mixed pathology was found in many of the discordant cases. These results should be interpreted in the context of a relatively young onset study population. Older patient populations would be expected to have a higher prevalence of mixed pathology overall, potentially impacting both PIB (higher baseline prevalence of amyloid positivity in the population) and FDG (patterns reflecting cumulative impact of multiple pathologies), complicating interpretation.

We identified several possible explanations for false positive and false negative PET scans. Positive PIB in the setting of low ADNC may be explained by high amyloid burden with low Braak stages of tau pathology corresponding with low ADNC. Corticobasal degeneration, which shows anatomic overlap with AD (particularly in parietal cortex, and to some degree in dorsolateral prefrontal regions) accounted for some cases of false positive FDG. Additional factors that were associated with incongruence between PET and autopsy included longer PET-to-autopsy intervals and mixed pathologies.

Tau PET tracers, currently being validated in the research setting[53] and recently approved for clinical use in the USA,[54] have the potential to complement amyloid PET and provide a more comprehensive in vivo characterization of AD neuropathology. The topography of tau PET shows a much tighter relationship with AD disease stage and clinical phenotype,[28,55] and thus merges the major strengths of amyloid PET (biochemical specificity for AD-related neuropathological changes) with those of FDG (anatomic specificity and clinical relevance). Early research suggests that tau PET patterns overlap with and precede hypometabolism on FDG.[28,56] Most currently available tau tracers show relative specificity for AD-related neurofibrillary tangles compared with tau aggregates in non-AD tauopathies, and thus may also be well suited for differential diagnosis.[57] Further work is needed to clarify the clinical role of tau PET as a complement to, or substitute for, amyloid and FDG PET.

Our study has several strengths. We studied a relatively large cohort of patients with antemortem PET and neuropathology. All patients were studied with both PET modalities, enabling a head-to-head comparison of PIB and FDG versus neuropathology as the gold standard. The clinical populations were more representative of cognitively impaired patients studied at academic centers (early stage, heterogeneous, and complex clinical presentations) than those included in previous PET-to-autopsy studies of amyloid PET (primarily end-of-life patients). We were able to further assess the utility of PIB and FDG in relevant clinical subgroups and provide recommendations for specific high-value clinical scenarios.

This study has limitations. First, the cohort is enriched for early age-at-onset dementia and FTD and underrepresents Lewy body dementia (LBD) and vascular cognitive impairment, which are common causes of late onset dementia. Nevertheless, the cohort is aligned with the strengths of both amyloid and FDG PET in differentiating AD and FTD and assessing early onset dementia. LBD and AD may be better differentiated by dopamine transporter imaging,[58] whereas vascular contributions to cognitive decline are best assessed by MRI.[59] Second, PET scan raters were not blinded to the primary research populations evaluated at our center, which may have introduced bias into their visual interpretations. Furthermore, neuropathologists reviewed clinical notes, which may have affected judgment about attribution of neuropathology as "primary" or "contributing," although this should not affect the staging of ADNC. Third, our cohort lacked racial and ethnic diversity. Fourth, amyloid PET was performed with PIB, a tracer that is not approved for clinical use or widely available outside the research setting due to the short half-life of the ^{11}C radioisotope. Previous

studies found similar retention characteristics and good visual read concordance comparing PIB and ^{18}F amyloid PET tracers, which have received regulatory approval for clinical use.[60–63] In this work, we specifically compared the accuracy of PIB and FDG in detecting AD pathology. Fifth, PET-to-autopsy interval in our study was on average relatively long (4.4 years). In secondary analyses evaluating the impact of PET-to-autopsy interval, we found that PIB and FDG performed equally well in shorter PET-to-autopsy intervals, whereas PIB had higher sensitivity in longer intervals, supporting its potential for early diagnosis. Sixth, the estimated values for positive and negative predictive values and accuracy are directly related to the prevalence of the disease in the study cohort. Finally, we assessed the performance of PIB and FDG imaging as standalone measures. The added value of PIB and FDG on the physician's clinical impression was not assessed here and should be the subject of future studies.

In summary, both amyloid and FDG PET showed high accuracy in detecting AD pathology, although PIB had higher sensitivity and negative predictive value, particularly in early disease stages. PIB and FDG performed comparably in identifying AD as the primary etiologic pathology underlying clinical impairment. When PIB and FDG were congruent, sensitivity, specificity, and total accuracy approached 100%. When scans were incongruent, mixed pathology was often found. PIB and FDG are both valuable PET tracers in the clinical assessment of cognitive decline, and the choice of modality can be well tailored to answer the specific clinical question.

Author Contributions

O.H.L.-S., R.L.J., and G.D.R. contributed to the conception and design of the study; all authors contributed to

the acquisition and analysis of data; O.H.L.-S., R.L.J., L.I., I.L., and G.D.R. contributed to drafting the text and preparing the figures.

Potential Conflicts of Interest

References

1. Galton CJ, Patterson K, Xuereb JH, Hodges JR. Atypical and typical presentations of Alzheimer's disease: a clinical, neuropsychological, neuroimaging and pathological study of 13 cases. Brain J Neurol 2000;123:484–498.

2. Graham A, Davies R, Xuereb J, et al. Pathologically proven frontotemporal dementia presenting with severe amnesia. Brain J Neurol 2005;128:597–605.

3. Boyle PA, Yu L, Leurgans SE, et al. Attributable risk of Alzheimer's dementia attributed to age-related neuropathologies. Ann Neurol 2019;85:114–124.

4. Beach TG, Monsell SE, Phillips LE, Kukull W. Accuracy of the clinical diagnosis of Alzheimer disease at National Institute on Aging Alzheimer Disease Centers, 2005-2010. J Neuropathol Exp Neurol 2012;71:266–273.

5. Seo SW, Ayakta N, Grinberg LT, et al. Regional correlations between [11C]PIB PET and post-mortem burden of amyloid-beta pathology in a diverse neuropathological cohort. Neuroimage Clin 2017;13:130–137.

6. Lowe VJ, Lundt ES, Albertson SM, et al. Neuroimaging correlates with neuropathologic schemes in neurodegenerative disease. Alzheimers Dement 2019;15:927–939.

7. Montine TJ, Phelps CH, Beach TG, et al. National Institute on Aging-Alzheimer's Association guidelines for the neuropathologic assessment of Alzheimer's disease: a practical approach. Acta Neuropathol 2012;123:1–11.

8. Minoshima S, Giordani B, Berent S, et al. Metabolic reduction in the posterior cingulate cortex in very early Alzheimer's disease. Ann Neurol 1997;42:85–94.

9. Foster NL, Heidebrink JL, Clark CM, et al. FDG-PET improves accuracy in distinguishing frontotemporal dementia and Alzheimer's disease. Brain J Neurol 2007;130:2616–2635.

10. Silverman DH, Small GW, Chang CY, et al. Positron emission tomography in evaluation of dementia: regional brain metabolism and long-term outcome. JAMA 2001;286:2120–2127.

11. Jagust W, Reed B, Mungas D, et al. What does fluorodeoxyglucose PET imaging add to a clinical diagnosis of dementia? Neurology 2007;69:871–877.

12. Bischof GN, Jessen F, Fliessbach K, et al. Impact of tau and amyloid burden on glucose metabolism in Alzheimer's disease. Ann Clin Transl Neurol 2016;3:934–939.

13. Clark CM, Pontecorvo MJ, Beach TG, et al. Cerebral PET with florbetapir compared with neuropathology at autopsy for detection of neuritic amyloid-β plaques: a prospective cohort study. Lancet Neurol 2012;11:669–678.

14. Sabri O, Sabbagh MN, Seibyl J, et al. Florbetaben PET imaging to detect amyloid beta plaques in Alzheimer's disease: phase 3 study. Alzheimers Dement 2015;11:964–974.

15. Curtis C, Gamez JE, Singh U, et al. Phase 3 trial of flutemetamol labeled with radioactive fluorine 18 imaging and neuritic plaque density. JAMA Neurol 2015;72:287–294.

16. La Joie R, Ayakta N, Seeley WW, et al. Multisite study of the relationships between antemortem [11C]PIB-PET centiloid values and post-mortem measures of Alzheimer's disease neuropathology. Alzheimers Dement 2019;15:205–216.

17. Rabinovici GD, Rosen HJ, Alkalay A, et al. Amyloid vs FDG-PET in the differential diagnosis of AD and FTLD. Neurology 2011;77:2034–2042.

18. Tolboom N, van der Flier WM, Boverhoff J, et al. Molecular imaging in the diagnosis of Alzheimer's disease: visual assessment of [11C]PIB and [18F]FDDNP PET images. J Neurol Neurosurg Psychiatry 2010;81:882–884.

19. Ng S, Villemagne VL, Berlangieri S, et al. Visual assessment versus quantitative assessment of 11C-PIB PET and 18F-FDG PET for detection of Alzheimer's disease. J Nucl Med 2007;48:547–552.

20. Fink HA, Linskens EJ, Silverman PC, et al. Accuracy of biomarker testing for neuropathologically defined Alzheimer disease in older adults with dementia. Ann Intern Med 2020;172:669–677.

21. Villeneuve S, Reed BR, Madison CM, et al. Vascular risk and Aβ interact to reduce cortical thickness in AD vulnerable brain regions. Neurology 2014;83:40–47.

22. Marchant NL, Reed BR, Sanossian N, et al. The aging brain and cognition: contribution of vascular injury and aβ to mild cognitive dysfunction. JAMA Neurol 2013;70:488–495.

23. Tsai RM, Bejanin A, Lesman-Segev O, et al. 18F-Flortaucipir (AV-1451) tau PET in frontotemporal dementia syndromes. Alzheimers Res Ther 2019;11:13.

24. Albert MS, DeKosky ST, Dickson D, et al. The diagnosis of mild cognitive impairment due to Alzheimer's disease: recommendations from the National Institute on Aging-Alzheimer's Association workgroups on diagnostic guidelines for Alzheimer's disease. Alzheimers Dement 2011;7:270–279.

25. McKhann GM, Knopman DS, Chertkow H, et al. The diagnosis of dementia due to Alzheimer's disease: recommendations from the National Institute on Aging-Alzheimer's Association workgroups on diagnostic guidelines for Alzheimer's disease. Alzheimers Dement 2011;7:263–269.

26. Lehmann M, Ghosh PM, Madison C, et al. Diverging patterns of amyloid deposition and hypometabolism in clinical variants of probable Alzheimer's disease. Brain 2013;136:844–858.

27. Lehmann M, Ghosh PM, Madison C, et al. Greater medial temporal hypometabolism and lower cortical amyloid burden in ApoE4-positive AD patients. J Neurol Neurosurg Psychiatry 2014;85:266–273.

28. Ossenkoppele R, Schonhaut DR, Schöll M, et al. Tau PET patterns mirror clinical and neuroanatomical variability in Alzheimer's disease. Brain J Neurol 2016;139:1551–1567.

29. Maass A, Landau S, Baker SL, et al. Comparison of multiple tau-PET measures as biomarkers in aging and Alzheimer's disease. Neuroimage 2017;157:448–463.

30. La Joie R, Bejanin A, Fagan AM, et al. Associations between [18F]AV1451 tau PET and CSF measures of tau pathology in a clinical sample. Neurology 2018;90:e282–e290.

31. Brown RKJ, Bohnen NI, Wong KK, et al. Brain PET in suspected dementia: patterns of altered FDG metabolism. Radiographics 2014; 34:684–701.

32. Douglas VC, DeArmond SJ, Aminoff MJ, et al. Seizures in corticobasal degeneration: a case report. Neurocase 2009;15:352–356.

33. Tartaglia MC, Sidhu M, Laluz V, et al. Sporadic corticobasal syndrome due to FTLD-TDP. Acta Neuropathol 2010;119:365–374.

34. Forman MS, Farmer J, Johnson JK, et al. Frontotemporal dementia: clinicopathological correlations. Ann Neurol 2006;59:952–962.

35. Mackenzie IRA, Neumann M, Bigio EH, et al. Nomenclature and nosology for neuropathologic subtypes of frontotemporal lobar degeneration: an update. Acta Neuropathol 2010;119:1–4.

36. Hyman BT, Phelps CH, Beach TG, et al. National Institute on Aging–Alzheimer's Association guidelines for the neuropathologic assessment of Alzheimer's disease. Alzheimers Dement 2012;8:1–13.

37. Thal DR, Rüb U, Orantes M, Braak H. Phases of A beta-deposition in the human brain and its relevance for the development of AD. Neurology 2002;58:1791–1800.

38. Braak H, Alafuzoff I, Arzberger T, et al. Staging of Alzheimer disease-associated neurofibrillary pathology using paraffin sections and immunocytochemistry. Acta Neuropathol 2006;112:389–404.

39. Mirra SS, Heyman A, McKeel D, et al. The Consortium to Establish a Registry for Alzheimer's Disease (CERAD). Part II. Standardization of the neuropathologic assessment of Alzheimer's disease. Neurology 1991;41:479–486.

40. Stock C, Hielscher T. DTComPair: comparison of binary diagnostic tests in a paired study design. 2014. Available at: https://CRAN.R-project.org/package=DTComPair. Accessed September 11, 2020.

41. Kuhn M. Building predictive models in R using the caret package. J Stat Softw 2008;28:1–26.

42. Gu W, Pepe MS. Estimating the capacity for improvement in risk prediction with a marker. Biostatistics 2009;10:172–186.

43. Leisenring W, Alonzo T, Pepe MS. Comparisons of predictive values of binary medical diagnostic tests for paired designs. Biometrics 2000;56:345–351.

44. Thiele C, Hirschfeld G. cutpointr: improved estimation and validation of optimal cutpoints in R. arXiv:2002.09209 [stat.CO]. Published online February 21, 2020. Available at: http://arxiv.org/abs/2002.09209. Accessed September 11, 2020.

45. Frank E Harrell Jr. rms: regression modeling strategies. 2020. Available at: https://CRAN.R-project.org/package=rms. Accessed September 11, 2020.

46. Rabinovici GD, Gatsonis C, Apgar C, et al. Association of amyloid positron emission tomography with subsequent change in clinical management among Medicare beneficiaries with mild cognitive impairment or dementia. JAMA 2019;321:1286–1294.

47. Suemoto CK, Ferretti-Rebustini REL, Rodriguez RD, et al. Neuropathological diagnoses and clinical correlates in older adults in Brazil: a cross-sectional study. PLoS Med 2017;14:e1002267.

48. Seeley WW, Crawford RK, Zhou J, et al. Neurodegenerative diseases target large-scale human brain networks. Neuron 2009;62:42–52.

49. Murray ME, Lowe VJ, Graff-Radford NR, et al. Clinicopathologic and 11C-Pittsburgh compound B implications of Thal amyloid phase across the Alzheimer's disease spectrum. Brain 2015;138:1370–1381.

50. Marshall GA, Fairbanks LA, Tekin S, et al. Early-onset Alzheimer's disease is associated with greater pathologic burden. J Geriatr Psychiatry Neurol 2007;20:29–33.

51. Ossenkoppele R, Jansen WJ, Rabinovici GD, et al. Prevalence of amyloid PET positivity in dementia syndromes: a meta-analysis. JAMA 2015;313:1939–1950.

52. Johnson KA, Minoshima S, Bohnen NI, et al. Appropriate use criteria for amyloid PET: a report of the Amyloid Imaging Task Force, the Society of Nuclear Medicine and Molecular Imaging, and the Alzheimer's Association. Alzheimers Dement 2013;9:e-1–e-16.

53. Villemagne VL, Fodero-Tavoletti MT, Masters CL, Rowe CC. Tau imaging: early progress and future directions. Lancet Neurol 2015;14:114–124.

54. Fleisher AS, Pontecorvo MJ, Devous MD, et al. Positron emission tomography imaging with [18F]flortaucipir and postmortem assessment of Alzheimer disease neuropathologic changes. JAMA Neurol 2020;77:829–839.

55. Bejanin A, Schonhaut DR, La Joie R, et al. Tau pathology and neurodegeneration contribute to cognitive impairment in Alzheimer's disease. Brain J Neurol 2017;140:3286–3300.

56. Ossenkoppele R, Iaccarino L, Schonhaut DR, et al. Tau covariance patterns in Alzheimer's disease patients match intrinsic connectivity networks in the healthy brain. Neuroimage Clin 2019;23:101848.

57. Ossenkoppele R, Rabinovici GD, Smith R, et al. Discriminative accuracy of [18F]flortaucipir positron emission tomography for Alzheimer disease vs other neurodegenerative disorders. JAMA 2018;320:1151–1162.

58. Thomas AJ, Attems J, Colloby SJ, et al. Autopsy validation of 123I-FP-CIT dopaminergic neuroimaging for the diagnosis of DLB. Neurology 2017;88:276–283.

59. Gorelick PB, Scuteri A, Black SE, et al. Vascular contributions to cognitive impairment and dementia: a statement for healthcare professionals from the American Heart Association/American Stroke Association. Stroke 2011;42:2672–2713.

60. Mountz JM, Laymon CM, Cohen AD, et al. Comparison of qualitative and quantitative imaging characteristics of [11C]PiB and [18F]flutemetamol in normal control and Alzheimer's subjects. Neuroimage Clin 2015;9:592–598.

61. Wolk DA, Zhang Z, Boudhar S, et al. Amyloid imaging in Alzheimer's disease: comparison of florbetapir and Pittsburgh compound-B positron emission tomography. J Neurol Neurosurg Psychiatry 2012;83:923–926.

62. Landau SM, Thomas BA, Thurfjell L, et al. Amyloid PET imaging in Alzheimer's disease: a comparison of three radiotracers. Eur J Nucl Med Mol Imaging 2014;41:1398–1407.

63. Villemagne VL, Mulligan RS, Pejoska S, et al. Comparison of 11C-PiB and 18F-florbetaben for Aβ imaging in ageing and Alzheimer's disease. Eur J Nucl Med Mol Imaging 2012;39:983–989.